A

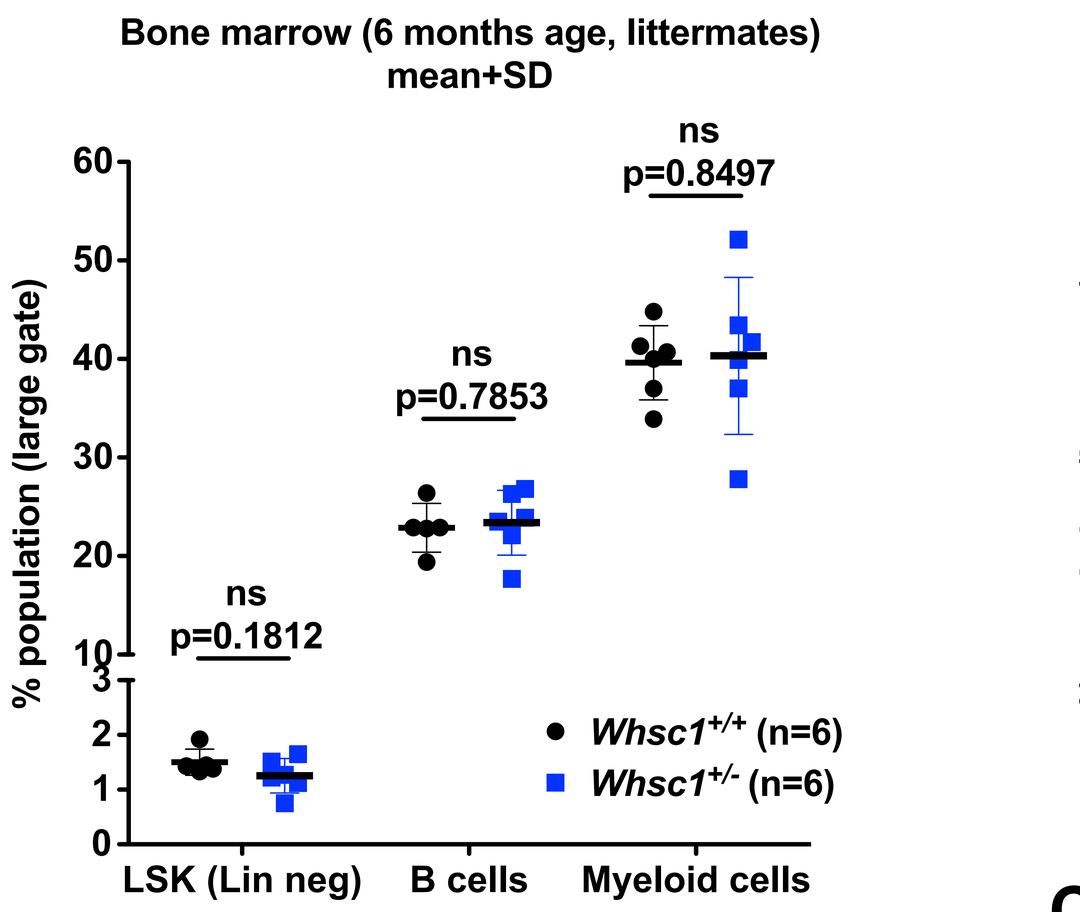
Bone marrow (6 months age, littermates)
mean+SD
% population (large gate)
ns
p=0.1812
ns
p=0.7853
ns
p=0.8497
Whsc1+/+ (n=6)
Whsc1+/- (n=6)
LSK (Lin neg)
B cells
Myeloid cells

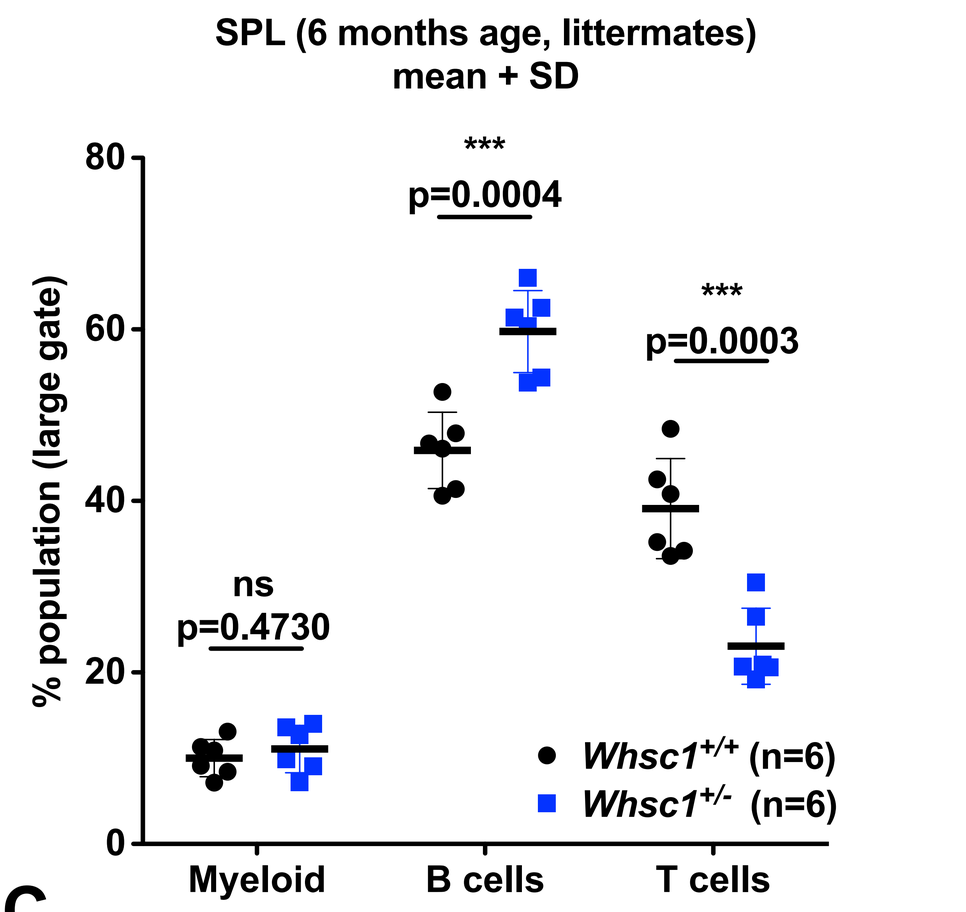
SPL (6 months age, littermates)
mean + SD
% population (large gate)
ns
p=0.4730
***
p=0.0004
***
p=0.0003
Whsc1+/+ (n=6)
Whsc1+/- (n=6)
Myeloid
B cells
T cells

B

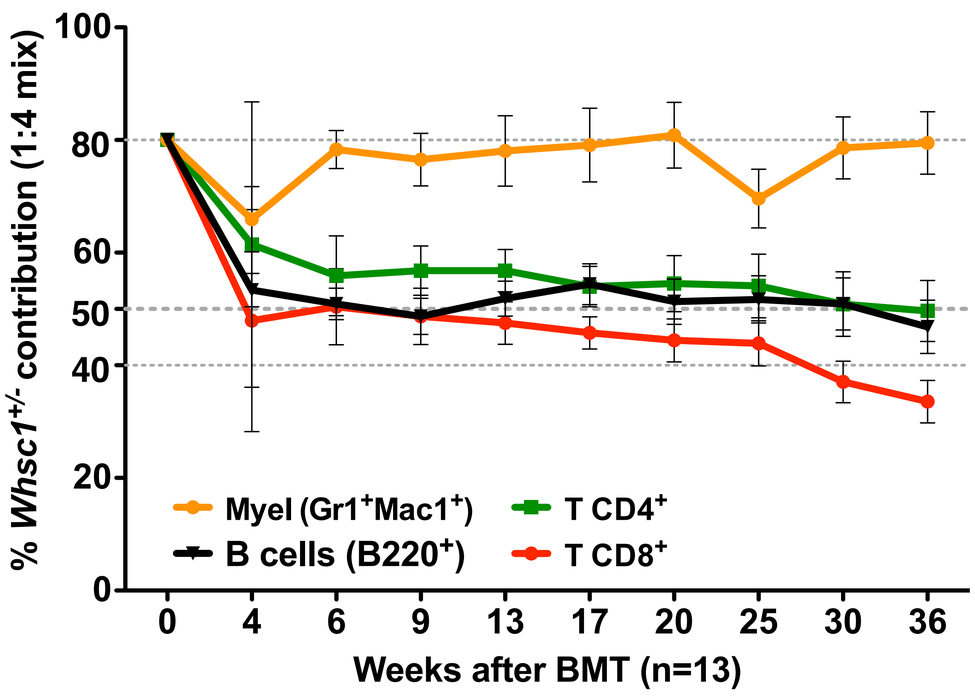
% Whsc1+/- contribution (1:4 mix)
Myel (Gr1+Mac1+)
B cells (B220+)
T CD4+
T CD8+
Weeks after BMT (n=13)

C

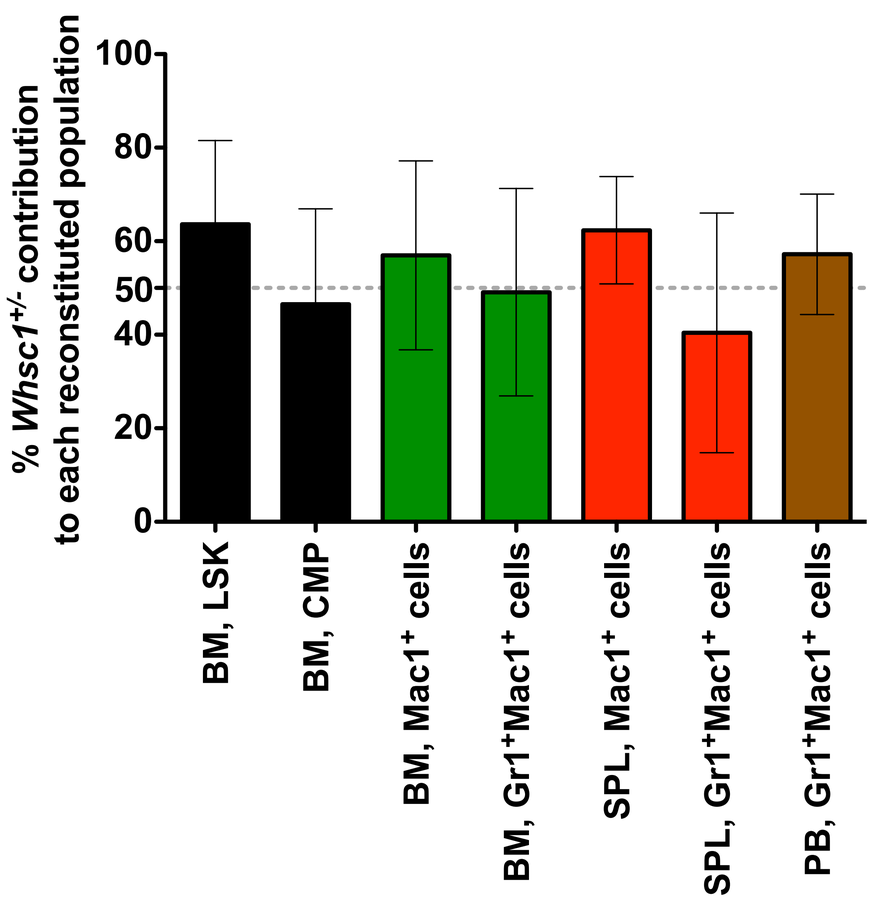
% Whsc1+/- contribution
to each reconstituted population
BM, LSK
BM, CMP
BM, Mac1+ cells
BM, Gr1+Mac1+ cells
SPL, Mac1+ cells
SPL, Gr1+Mac1+ cells
PB, Gr1+Mac1+ cells

D

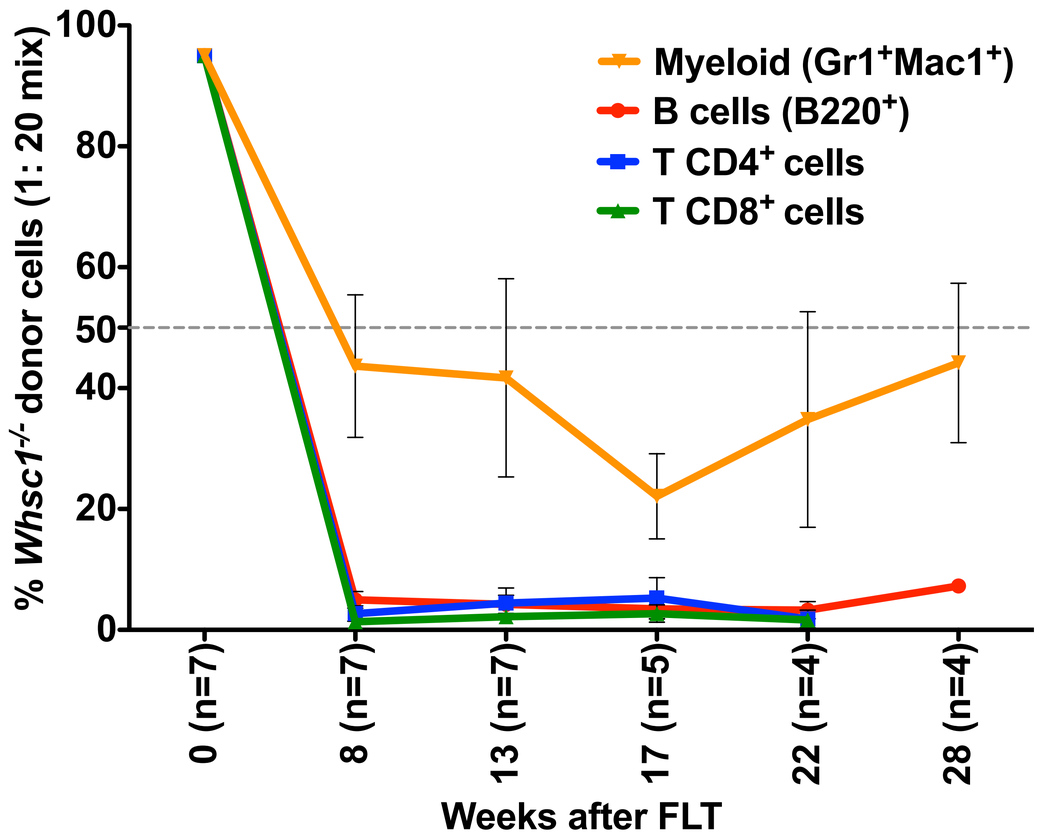
% Whsc1-/- donor cells (1: 20 mix)
Myeloid (Gr1+Mac1+)
B cells (B220+)
T CD4+ cells
T CD8+ cells
0 (n=7)
8 (n=7)
13 (n=7)
17 (n=5)
22 (n=4)
28 (n=4)
Weeks after FLT

E

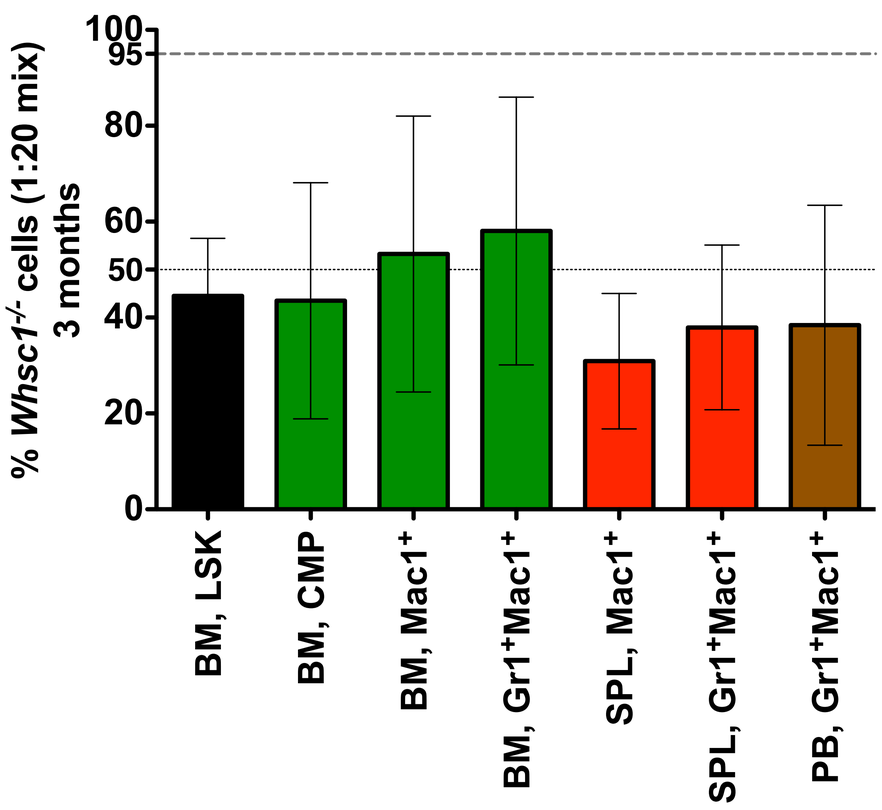
% Whsc1-/- cells (1:20 mix)
3 months
BM, LSK
BM, CMP
BM, Mac1+
BM, Gr1+Mac1+
SPL, Mac1+
SPL, Gr1+Mac1+
PB, Gr1+Mac1+

F

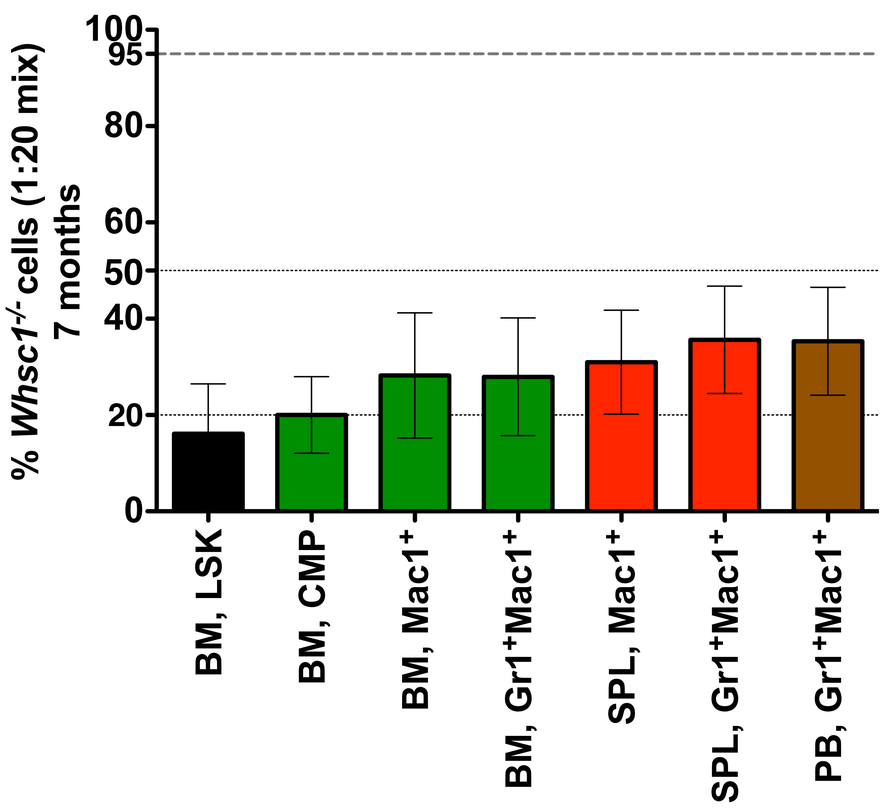
% Whsc1-/- cells (1:20 mix)
7 months
BM, LSK
BM, CMP
BM, Mac1+
BM, Gr1+Mac1+
SPL, Mac1+
SPL, Gr1+Mac1+
PB, Gr1+Mac1+

Figure S1 (related to Figure 1) (**A**) Absence of major alterations in the hematopoietic development of young *Whsc1*$^{+/-}$ mice. The graphs represent the percentages, as determined by FACS, of the indicated cellular populations in the BM (left) and spleen (right) of either WT (black circles) or *Whsc1*$^{+/-}$ (blue squares) 6 month-old littermate mice. A total of 6 WT and 6 *Whsc1*$^{+/-}$ mice were analyzed. p values refer to a two-sided Student's t test. (**B**) Rescue of the disadvantage of *Whsc1*$^{+/-}$ hematopoietic cells in a competitive BM reconstitution assay. The vertical axis shows the percentage of contribution of the indicated *Whsc1*$^{+/-}$ cell types to the peripheral blood of recipient mice injected with a 1:4 mix of WT:*Whsc1*$^{+/-}$ cells, as determined by flow cytometry of peripheral blood samples at the times indicated on the "x" axis. *Whsc1*$^{+/-}$ myeloid cells behave similarly to WT cells and are maintained at the ratio of injection, while the 5-fold impairment of *Whsc1*$^{+/-}$ cells (see also Figure 1B) can be rescued by increasing the percentage of competing cells. Mean ± SEM are shown. (**C**) Percentage of contribution of the indicated *Whsc1*$^{+/-}$ myeloid cell types to the indicated hematopoietic organs of recipient mice injected with a 1:1 mix of WT:*Whsc1*$^{+/-}$ cells, 3-6 months after injection. n = 5 mice for each time point. Mean ± SD are shown. (**D**) Vertical axis shows the drastically reduced percentage of contribution of the indicated *Whsc1*$^{-/-}$ cell types to the peripheral blood of recipient mice injected with either a 1:20 mix of WT:*Whsc1*$^{-/-}$ cells, as determined by flow cytometry of peripheral blood samples at the weeks indicated on the "x" axis. Mean ± SEM are shown. (**E, F**) Percentage of contribution of the indicated *Whsc1*$^{-/-}$ cell types to the indicated hematopoietic organs of recipient mice injected with a 1:20 mix of WT:*Whsc1*$^{-/-}$ cells, 3 (**E**) or 7 (**F**) months after injection. The panels show how myeloid compartments are unaffected relative to the BM LSK percentages. n = 2 or 5 mice (3 and 7 months, respectively). Mean ± SD are shown.

A

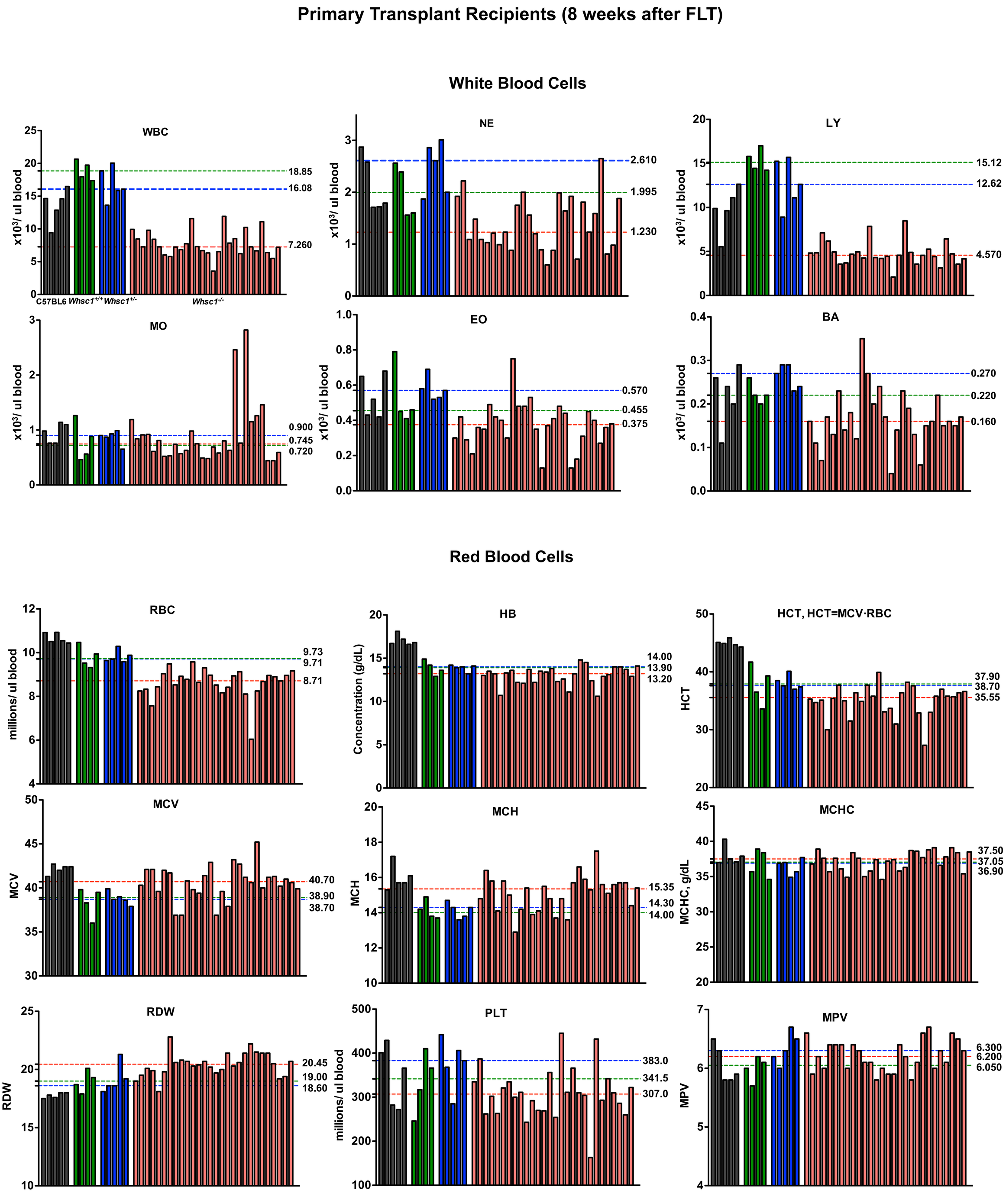
Primary Transplant Recipients (8 weeks after FLT)
White Blood Cells
WBC
x10³/ ul blood
18.85
16.08
7.260
C57BL6 Whsc1+/+ Whsc1+/- Whsc1-/-
NE
2.610
1.995
1.230
LY
15.12
12.62
4.570
MO
0.900
0.745
0.720
EO
0.570
0.455
0.375
BA
0.270
0.220
0.160
Red Blood Cells
RBC
millions/ ul blood
9.73
9.71
8.71
HB
Concentration (g/dL)
14.00
13.90
13.20
HCT, HCT=MCV·RBC
HCT
37.90
38.70
35.55
MCV
40.70
38.90
38.70
MCH
15.35
14.30
14.00
MCHC
MCHC, g/dL
37.50
37.05
36.90
RDW
20.45
19.00
18.60
PLT
millions/ ul blood
383.0
341.5
307.0
MPV
6.300
6.200
6.050

Figure S2 (related to Figure 1). Full hematimetric analysis of recipients of a primary fetal liver transplant, showing the absolute numbers of the different blood cell types. Non-transplanted, WT C57Bl/6 mice were used as controls (leftmost bars, in black). Each bar represents an individual mouse. Green, blue and red dotted lines represents the median value for *Whsc1*$^{+/+}$, *Whsc1*$^{+/-}$ and *Whsc1*$^{-/-}$ recipients, respectively.

Figure S3

Campos-Sanchez *et al.*

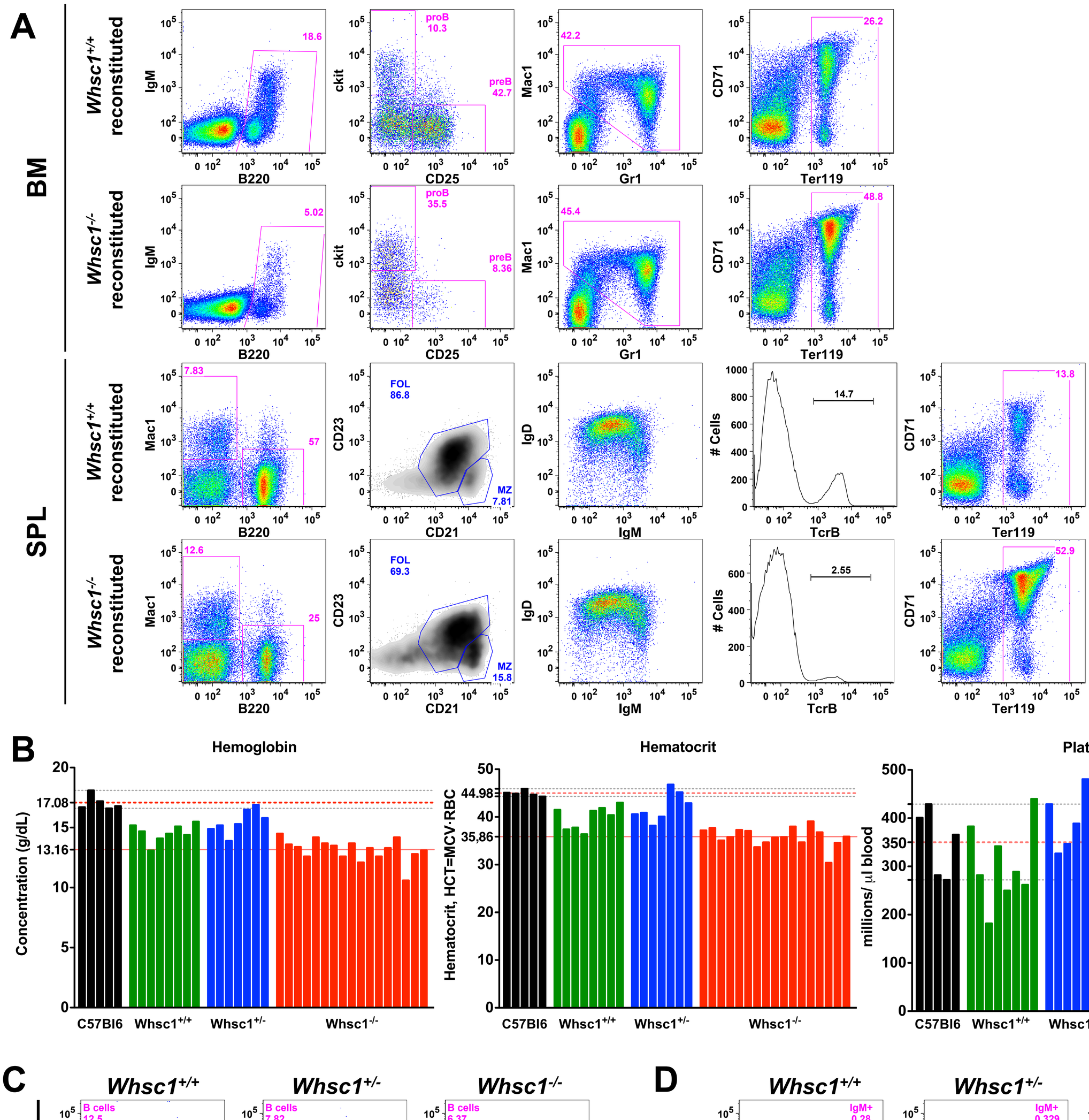

Figure S3 (related to Figures 1 and 3) (**A**) Representative FACS plots of hematopoietic organs from mice primary reconstituted with either WT or *Whsc1*$^{-/-}$ FL cells, 3-6 months after FL transplant. (**B**) Absolute numbers of total blood erythrocytes, hemoglobin, hematocrit and platelets from mice reconstituted with a secondary serial transplant of either *Whsc1*$^{+/+}$, *Whsc1*$^{+/-}$, or *Whsc1*$^{-/-}$ cells, 6 weeks after transplant, as measured by automatic hematic biometry. Non-transplanted, WT C57Bl/6 mice were used as controls (leftmost bars). (**C**) Strengthening of the developmental block beyond the proB cell stage and presence of increased splenic erythrocytes in secondary recipients of *Whsc1*$^{-/-}$ cells. BM of the recipients of the indicated genotypes was analyzed 6 months after transplant. Data shown are representative FACS plots, out of 6 independently analyzed *Whsc1*$^{-/-}$ recipients, 4 *Whsc1*$^{+/-}$ recipients, and 4 *Whsc1*$^{+/+}$ (**D**) Hematopoietic alterations in *Whsc1*$^{-/-}$ embryos. FACS analysis of fetal spleen (upper row) and fetal thymi (lower row) of *Whsc1*$^{-/-}$ E21 embryos and their WT and heterozygous littermates. Lower left graph: percentages of CD19^{+} cells in fetal spleens of the indicated genotypes. Lower right bar graph: percentages of CD4-SP T cells in fetal thymi of the indicated genotypes. n= number of embryos analyzed.

A

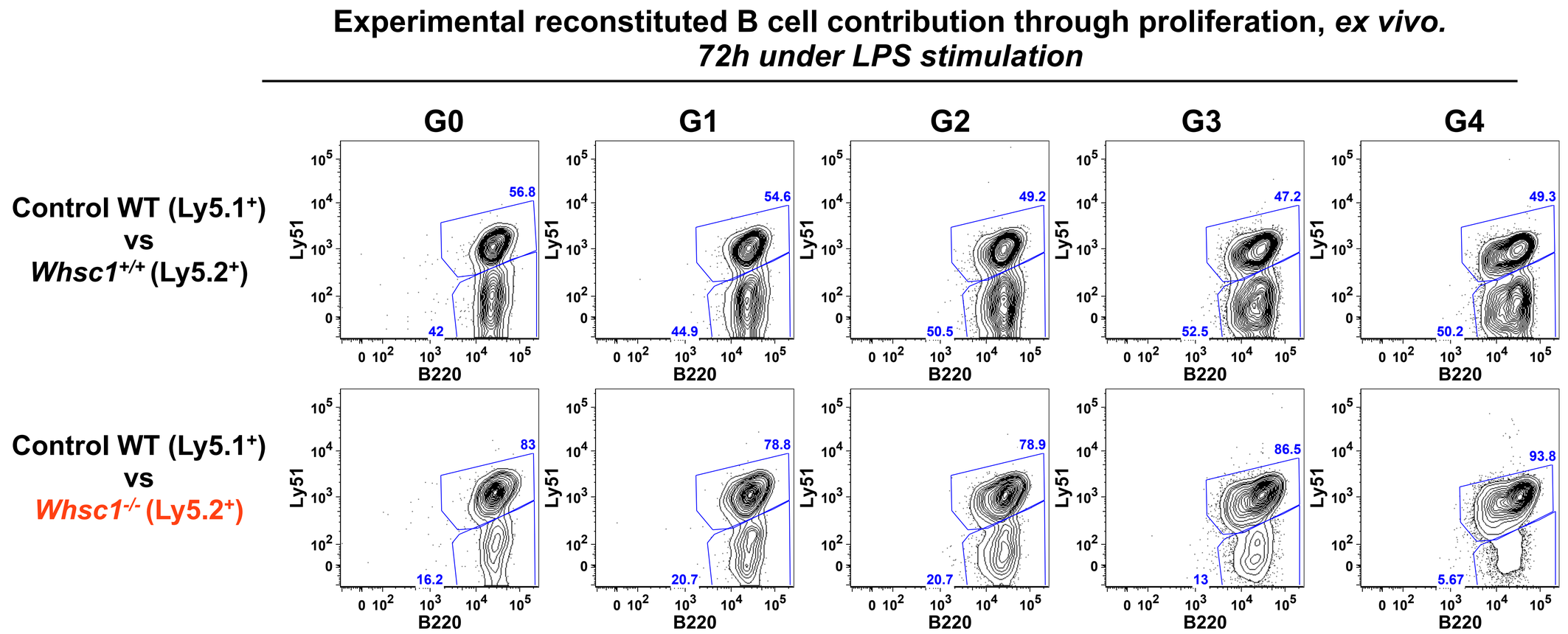
Experimental reconstituted B cell contribution through proliferation, ex vivo.
72h under LPS stimulation
G0
G1
G2
G3
G4
Control WT (Ly5.1+)
vs
Whsc1+/+ (Ly5.2+)
Control WT (Ly5.1+)
vs
Whsc1-/- (Ly5.2+)
Ly51
B220
56.8
42
54.6
44.9
49.2
50.5
47.2
52.5
49.3
50.2
83
16.2
78.8
20.7
78.9
20.7
86.5
13
93.8
5.67

B

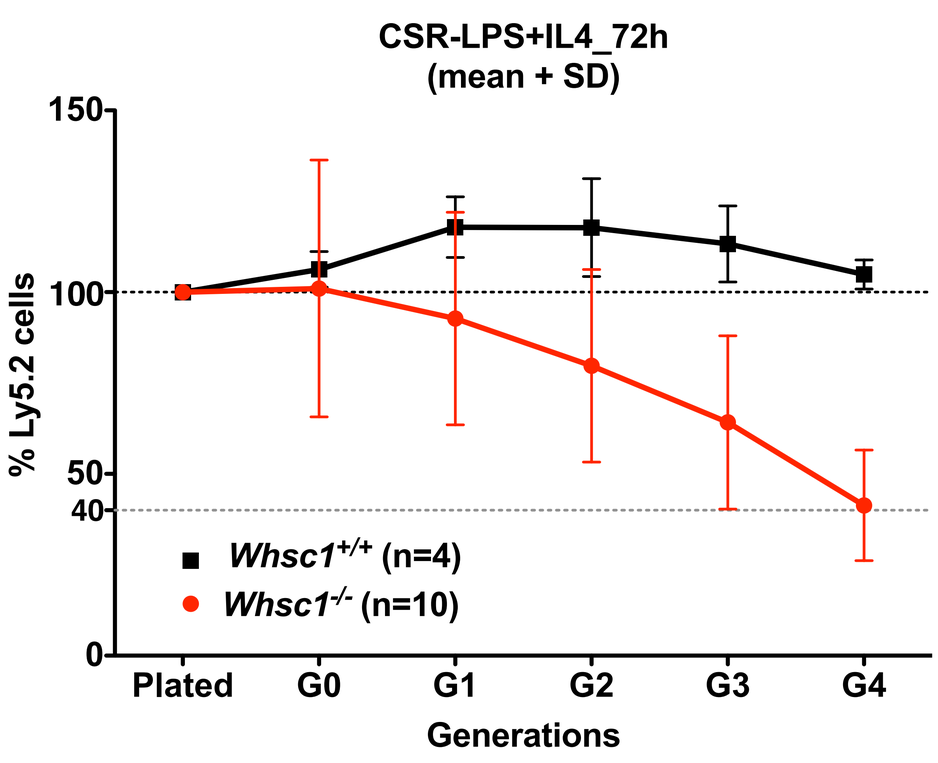
CSR-LPS+IL4_72h
(mean + SD)
% Ly5.2 cells
Whsc1+/+ (n=4)
Whsc1-/- (n=10)
Plated
G0
G1
G2
G3
G4
Generations

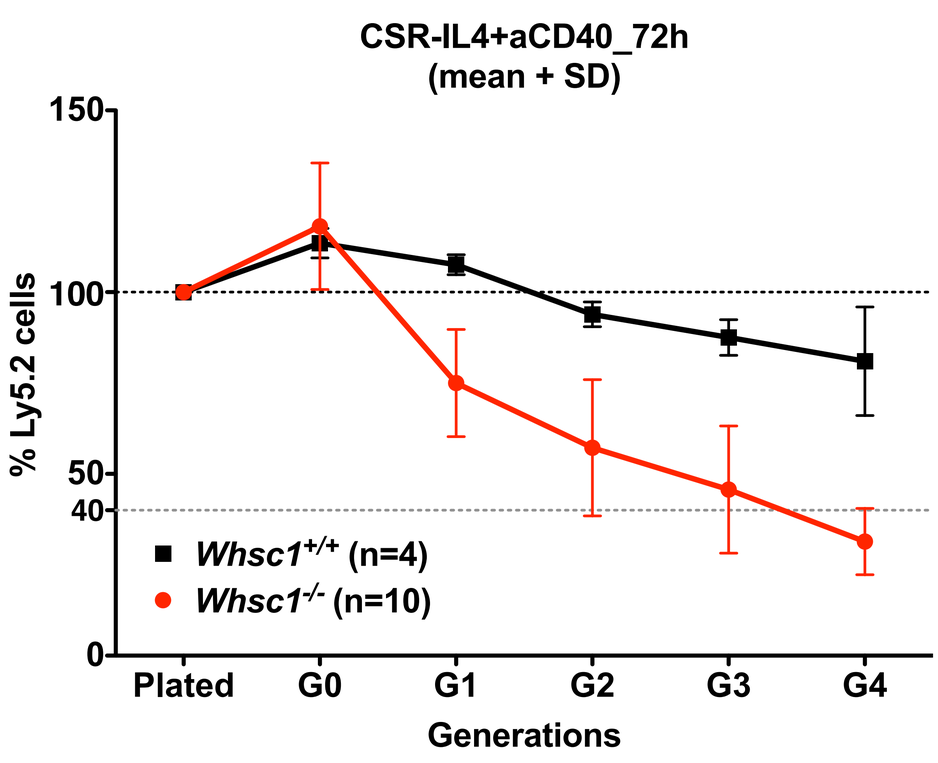
CSR-IL4+aCD40_72h
(mean + SD)
% Ly5.2 cells
Whsc1+/+ (n=4)
Whsc1-/- (n=10)
Plated
G0
G1
G2
G3
G4
Generations

Figure S4 (related to Figure 4) (**A**) Deconvolution of an ex vivo LPS-stimulation experiment, performed in competition, into the different cellular generations (G0 to G4) as identified by CellTrace dilution. The upper row shows a control experiment in which WT Ly5.1 cells compete with WT-reconstituted Ly5.2 cells, showing the even distribution of cells (approximately 50:50) throughout the generations. The lower row shows the competition of WT Ly5.1 cells with *Whsc1*$^{-/-}$ Ly5.2 cells (also 50:50), where the rapid and progressive reduction in the contribution of the latter can be clearly appreciated after 72 hours. (**B**) Evolution of the percentage of either WT or *Whsc1*$^{-/-}$ ex vivo stimulated Ly5.2 B cells, in competition against WT Ly5.1 B cells, along the different generations, and relative to the initial percentage when plated, with different stimulations. Mean ± SD are shown.

A

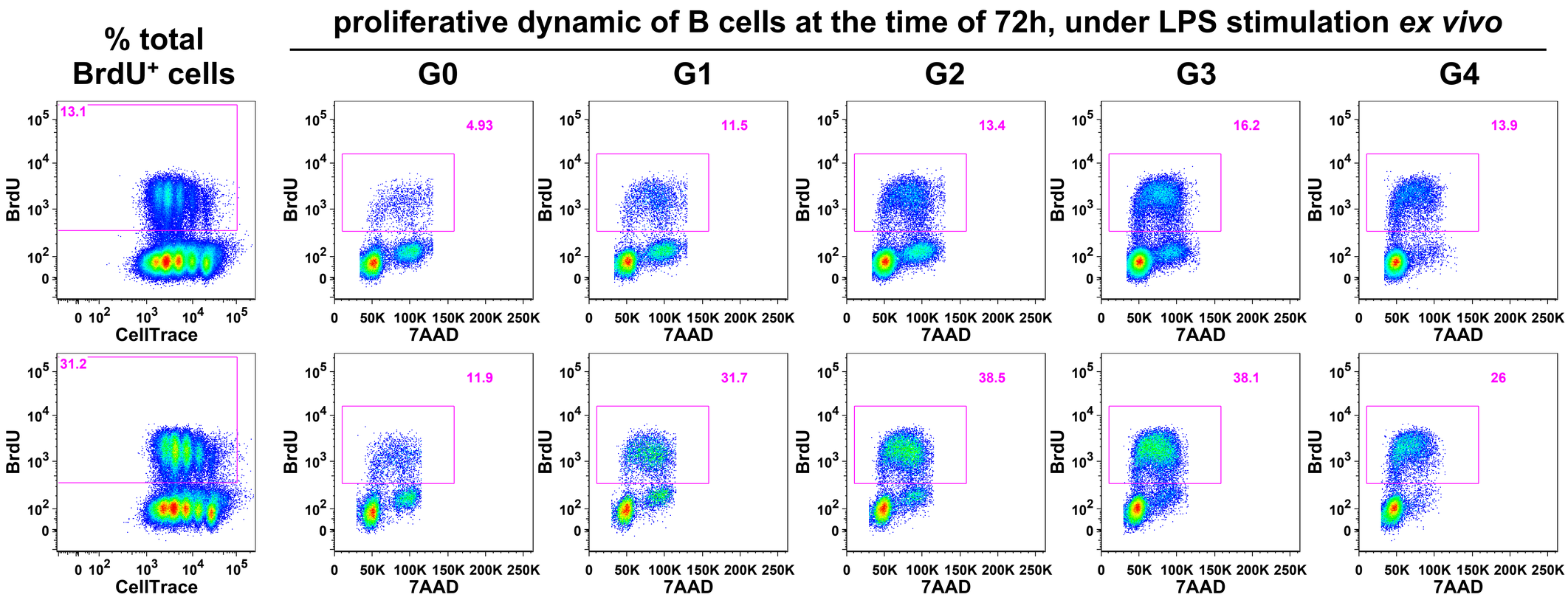
% total BrdU+ cells
proliferative dynamic of B cells at the time of 72h, under LPS stimulation ex vivo
G0
G1
G2
G3
G4
WT
Whsc1-/-
BrdU
CellTrace
7AAD
13.1
4.93
11.5
13.4
16.2
13.9
31.2
11.9
31.7
38.5
38.1
26

B

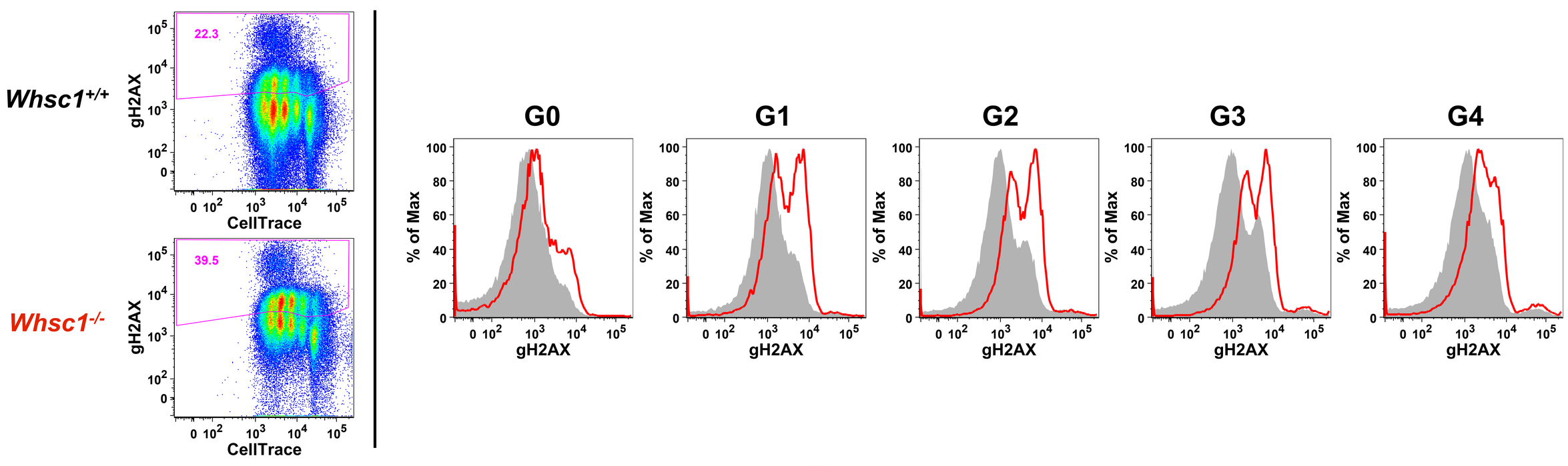
Whsc1+/+
Whsc1-/-
gH2AX
CellTrace
22.3
39.5
G0
G1
G2
G3
G4
% of Max
gH2AX

C

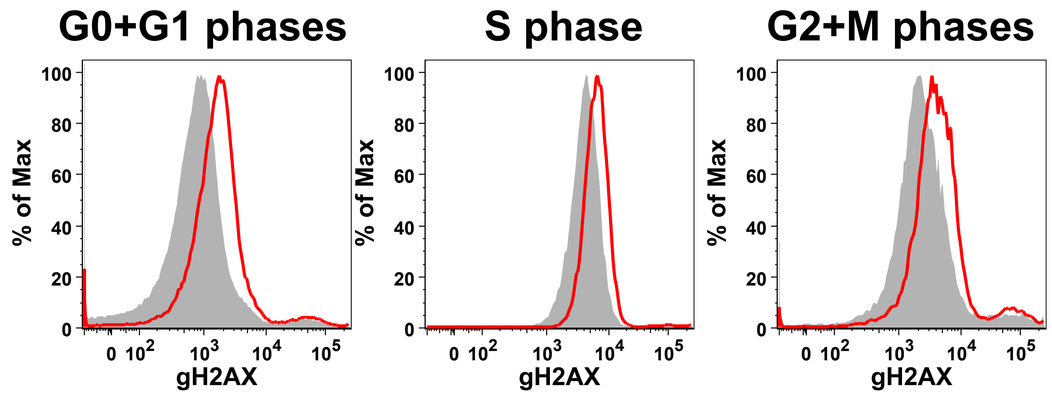
G0+G1 phases
S phase
G2+M phases
% of Max
gH2AX

D

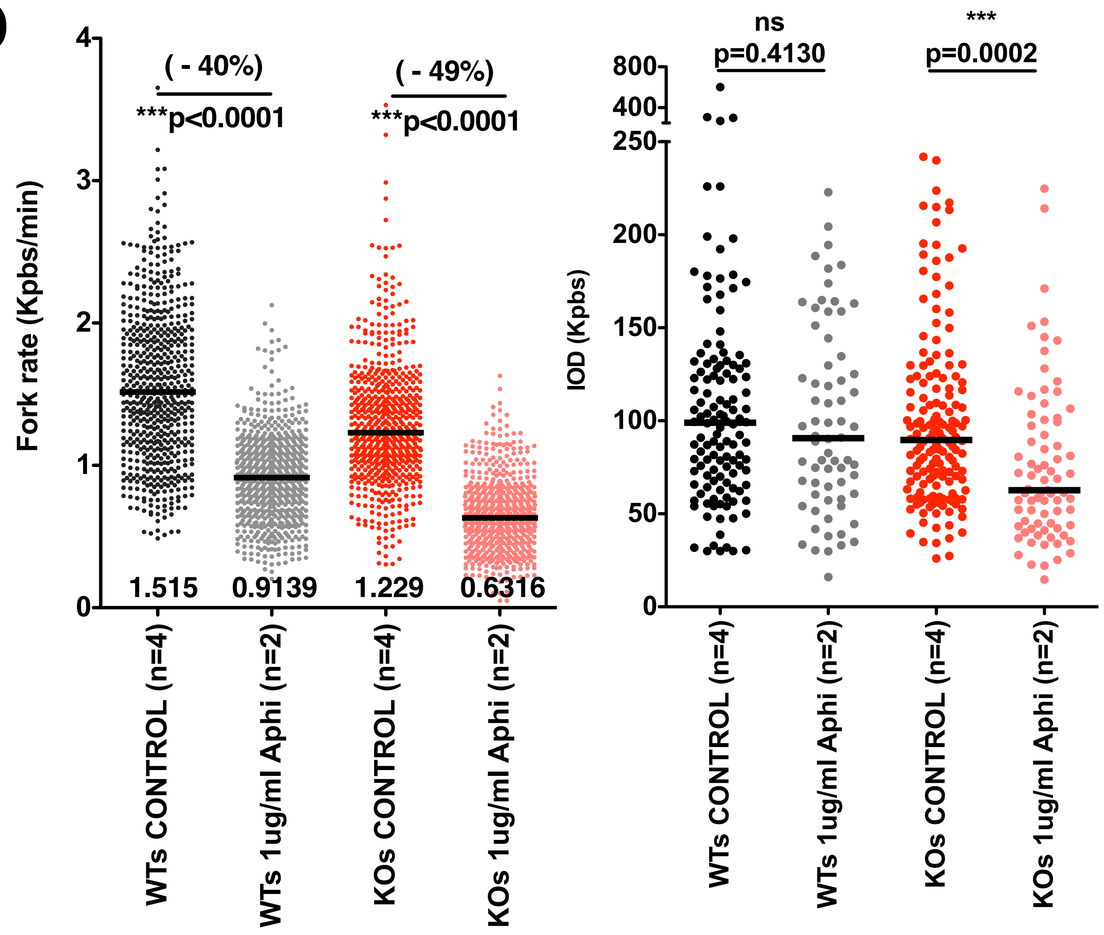
(- 40%)
***p<0.0001
(- 49%)
***p<0.0001
ns
p=0.4130
***
p=0.0002
Fork rate (Kpbs/min)
IOD (Kpbs)
1.515
0.9139
1.229
0.6316
WTs CONTROL (n=4)
WTs 1ug/ml Aphi (n=2)
KOs CONTROL (n=4)
KOs 1ug/ml Aphi (n=2)

E

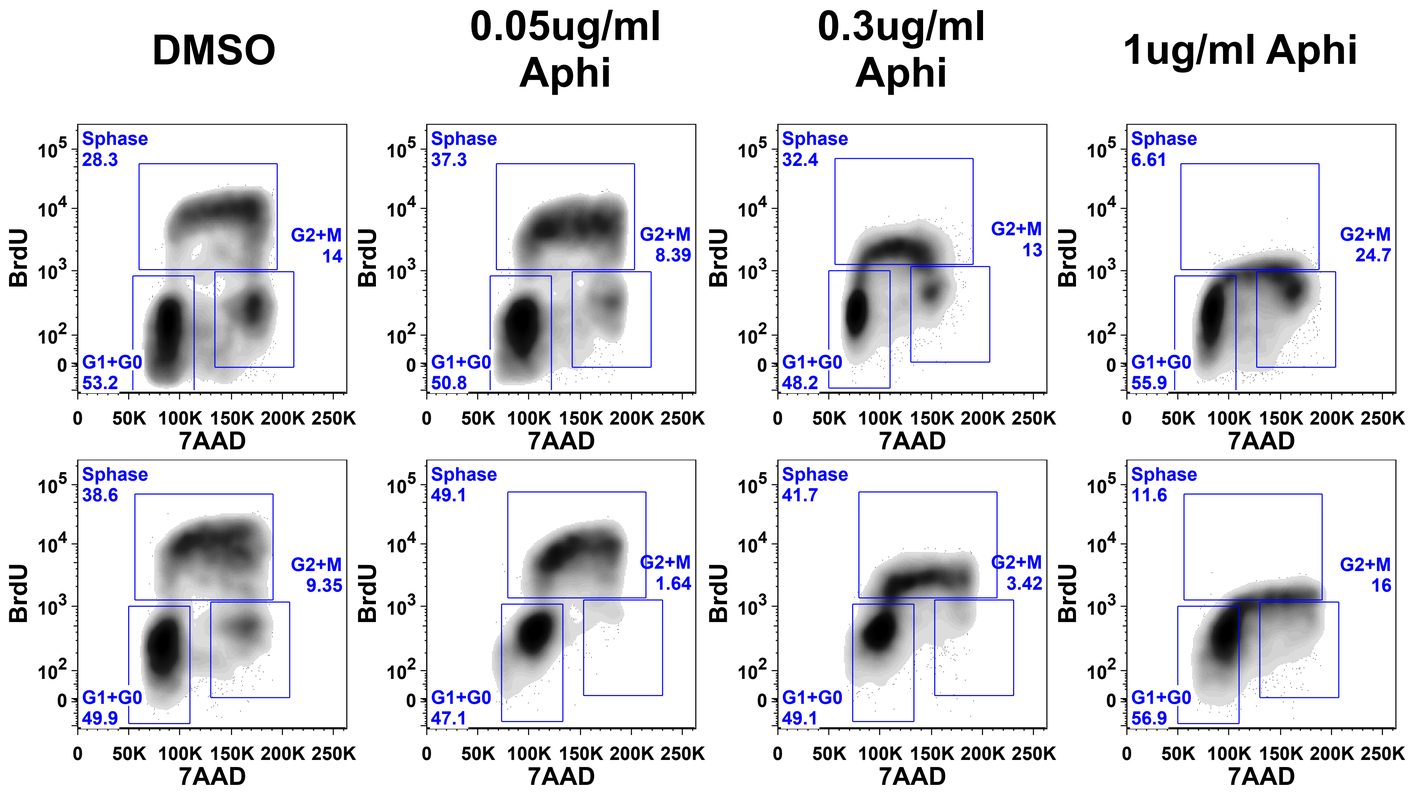
DMSO
0.05ug/ml Aphi
0.3ug/ml Aphi
1ug/ml Aphi
WT (n=2)
Whsc1-/- (n=2)
BrdU
7AAD
Sphase
G2+M
G1+G0
28.3
14
53.2
37.3
8.39
50.8
32.4
13
48.2
6.61
24.7
55.9
38.6
9.35
49.9
49.1
1.64
47.1
41.7
3.42
49.1
11.6
16
56.9

Figure S5 (related to Figures 5 and 6) (**A**) Deconvolution of the population of LPS-stimulated, BrdU-labelled B cells into the different generations according to the dilution of the CellTrace dye. Cell cycle profile (BrdU vs. 7AAD) are shown for all the different generations (G0-G4) of cells, showing the generalized 3-fold increased percentage of *Whsc1*$^{-/-}$ cells in the S phase. Representative plots of two out of 10 mice analyzed. Four representative panels from this figure were selected for display in main Figure 5a (**B**) Deconvolution of the population of LPS-stimulated B cells into the different generations according to the dilution of the CellTrace dye, showing the progressive accumulation of γH2AX in *Whsc1*$^{-/-}$ cells along all the different generations (G0-G4). Representative plots of two out of 7 mice analyzed. (**C**) Increased γH2AX accumulation is distributed throughout all the stages of cell cycle in LPS-stimulated *Whsc1*$^{-/-}$ B cells. (**D**) DNA fiber analysis of MEFs in the presence of aphidicolin. Fork rate (left panel) in Kbps/min, and Inter Origin Distance, (IOD, right panel) in Kpbs were measured for WT (black or grey) or *Whsc1*$^{-/-}$ (red or pink) MEFs in the absence (black or red) or presence (grey or pink) of aphidicolin. n= number of different clones. Horizontal bar represents the median for each data column. (**E**) Flow cytometry cell cycle analysis of LPS-stimulated WT or *Whsc1*$^{-/-}$ B cells in the presence of increasing concentrations of aphidicolin. To avoid interference with accumulating apoptotic cells in the total population, the plots represent the second generation of dividing cells, as deconvoluted using the CellTrace dilution signal. The experiment was repeated twice.

A

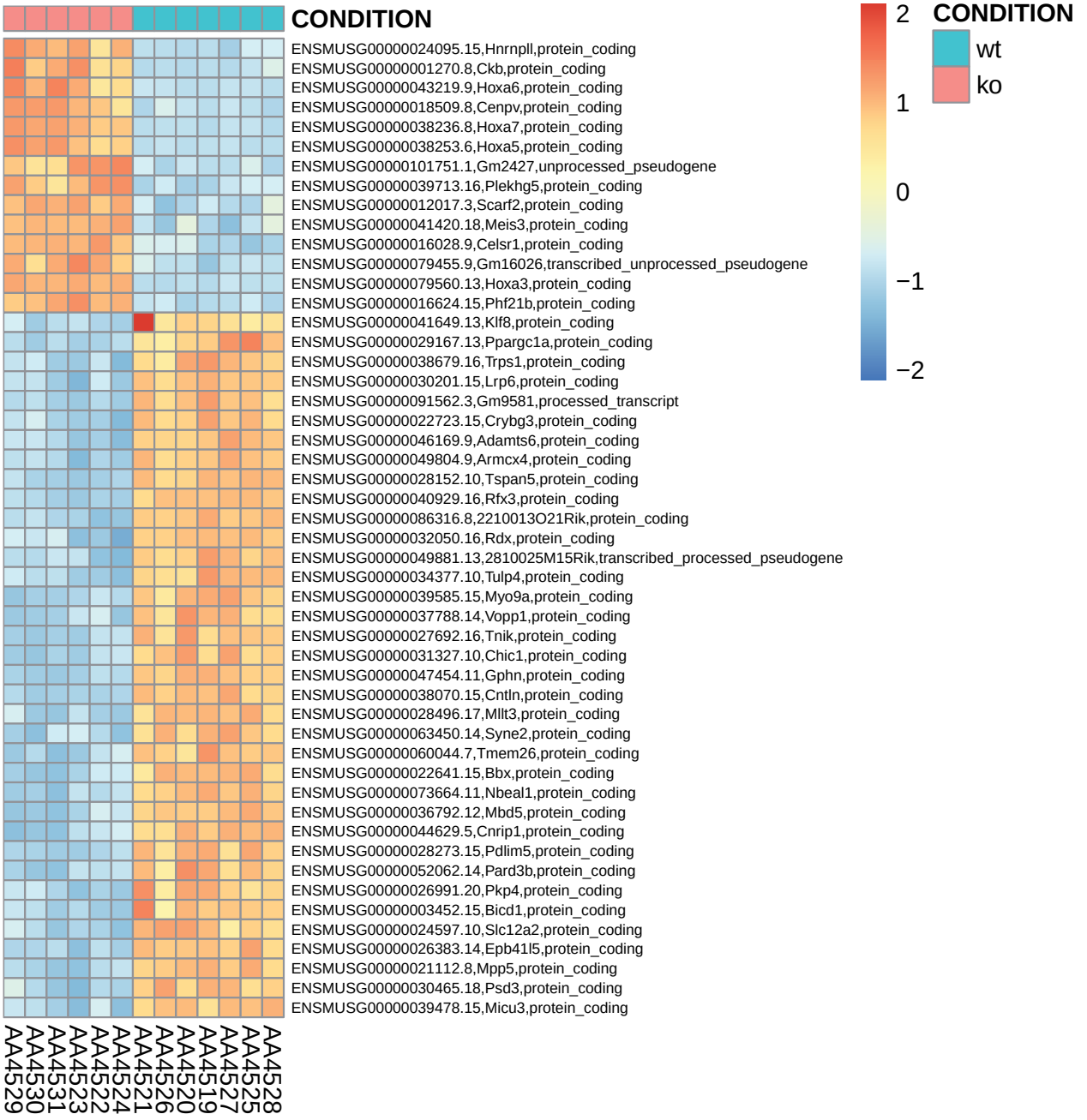
CONDITION
ENSMUSG00000024095.15,Hnrnpll,protein_coding
ENSMUSG00000001270.8,Ckb,protein_coding
ENSMUSG00000043219.9,Hoxa6,protein_coding
ENSMUSG00000018509.8,Cenpv,protein_coding
ENSMUSG00000038236.8,Hoxa7,protein_coding
ENSMUSG00000038253.6,Hoxa5,protein_coding
ENSMUSG00000101751.1,Gm2427,unprocessed_pseudogene
ENSMUSG00000039713.16,Plekhg5,protein_coding
ENSMUSG00000012017.3,Scarf2,protein_coding
ENSMUSG00000041420.18,Meis3,protein_coding
ENSMUSG00000016028.9,Celsr1,protein_coding
ENSMUSG00000079455.9,Gm16026,transcribed_unprocessed_pseudogene
ENSMUSG00000079560.13,Hoxa3,protein_coding
ENSMUSG00000016624.15,Phf21b,protein_coding
ENSMUSG00000041649.13,Klf8,protein_coding
ENSMUSG00000029167.13,Ppargc1a,protein_coding
ENSMUSG00000038679.16,Trps1,protein_coding
ENSMUSG00000030201.15,Lrp6,protein_coding
ENSMUSG00000091562.3,Gm9581,processed_transcript
ENSMUSG00000022723.15,Crybg3,protein_coding
ENSMUSG00000046169.9,Adamts6,protein_coding
ENSMUSG00000049804.9,Armcx4,protein_coding
ENSMUSG00000028152.10,Tspan5,protein_coding
ENSMUSG00000040929.16,Rfx3,protein_coding
ENSMUSG00000086316.8,2210013O21Rik,protein_coding
ENSMUSG00000032050.16,Rdx,protein_coding
ENSMUSG00000049881.13,2810025M15Rik,transcribed_processed_pseudogene
ENSMUSG00000034377.10,Tulp4,protein_coding
ENSMUSG00000039585.15,Myo9a,protein_coding
ENSMUSG00000037788.14,Vopp1,protein_coding
ENSMUSG00000027692.16,Tnik,protein_coding
ENSMUSG00000031327.10,Chic1,protein_coding
ENSMUSG00000047454.11,Gphn,protein_coding
ENSMUSG00000038070.15,Cntln,protein_coding
ENSMUSG00000028496.17,Mllt3,protein_coding
ENSMUSG00000063450.14,Syne2,protein_coding
ENSMUSG00000060044.7,Tmem26,protein_coding
ENSMUSG00000022641.15,Bbx,protein_coding
ENSMUSG00000073664.11,Nbeal1,protein_coding
ENSMUSG00000036792.12,Mbd5,protein_coding
ENSMUSG00000044629.5,Cnrip1,protein_coding
ENSMUSG00000028273.15,Pdlim5,protein_coding
ENSMUSG00000052062.14,Pard3b,protein_coding
ENSMUSG00000026991.20,Pkp4,protein_coding
ENSMUSG00000003452.15,Bicd1,protein_coding
ENSMUSG00000024597.10,Slc12a2,protein_coding
ENSMUSG00000026383.14,Epb41l5,protein_coding
ENSMUSG00000021112.8,Mpp5,protein_coding
ENSMUSG00000030465.18,Psd3,protein_coding
ENSMUSG00000039478.15,Micu3,protein_coding
AA4529
AA4530
AA4531
AA4523
AA4522
AA4524
AA4521
AA4526
AA4520
AA4519
AA4527
AA4525
AA4528
2
1
0
−1
−2
CONDITION
wt
ko

Figure S6 (1st part) (related to Figure 6) Differential expression analyses based on RNA-seq experiments of GC B cells. (**A**) Heatmap of the top 50 Differentially Expressed genes between WT and *Whsc1*$^{-/-}$ cells. (see Figure 6B).

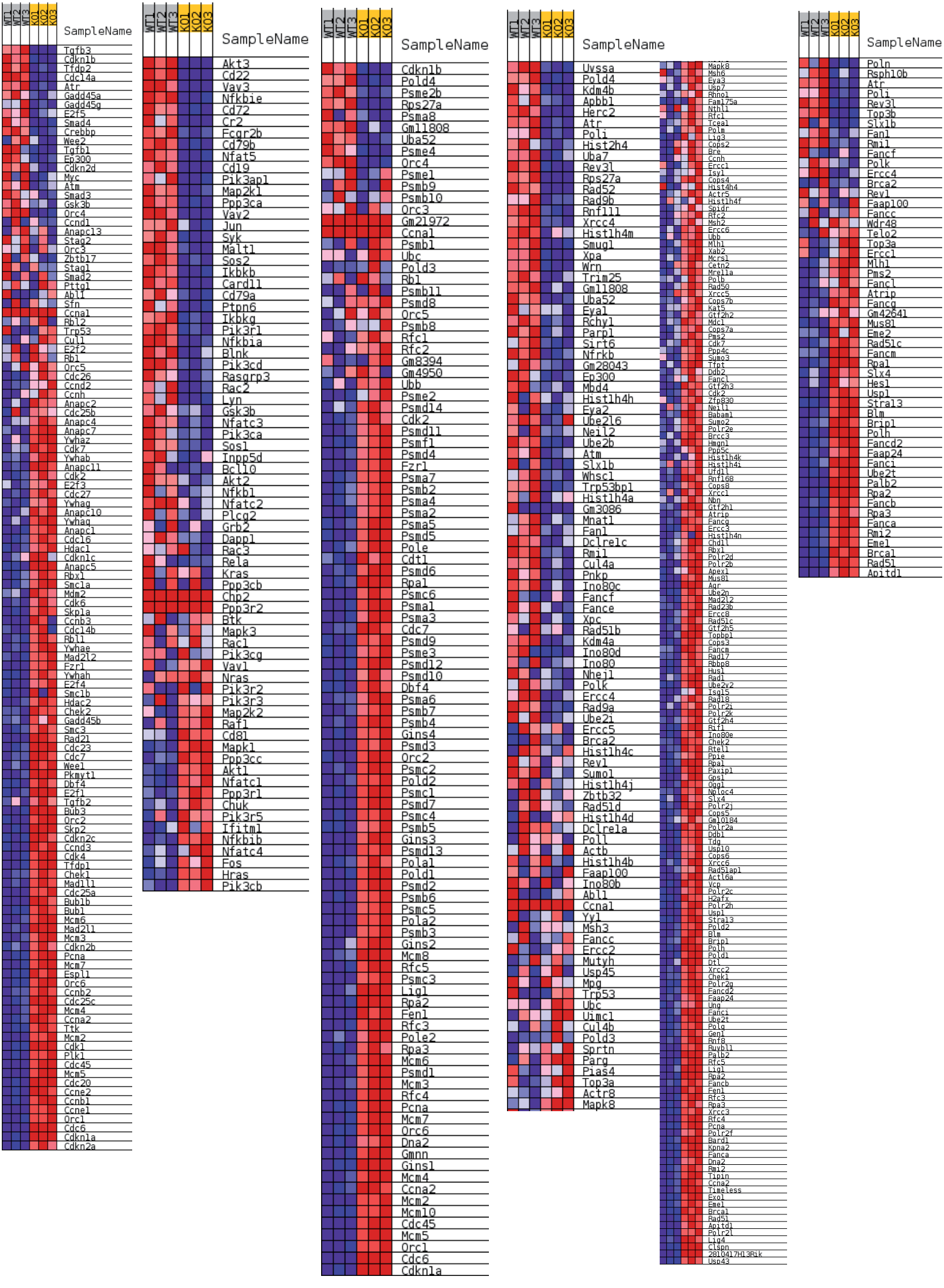
CELL CYCLE
BCR_SIGNALLING
DNA REPLICATION
DNA REPAIR
DNA REPAIR (cont)
FANCONI ANEM.
WT1
WT2
WT3
KO1
KO2
KO3
SampleName
Tgfb3
Cdkn1b
Tfdp2
Cdc14a
Atr
Gadd45a
Gadd45g
E2f5
Smad4
Crebbp
Wee2
Tgfb1
Ep300
Cdkn2d
Myc
Atm
Smad3
Gsk3b
Orc4
Ccnd1
Anapc13
Stag2
Orc3
Zbtb17
Stag1
Smad2
Pttg1
Abl1
Sfn
Ccna1
Rbl2
Trp53
Cul1
E2f2
Rb1
Orc5
Cdc26
Ccnd2
Ccnh
Anapc2
Cdc25b
Anapc4
Anapc7
Ywhaz
Cdk7
Ywhab
Anapc11
Cdk2
E2f3
Cdc27
Ywhag
Anapc10
Ywhaq
Anapc1
Cdc16
Hdac1
Cdkn1c
Anapc5
Rbx1
Smc1a
Mdm2
Cdk6
Skp1a
Ccnb3
Cdc14b
Rbl1
Ywhae
Mad2l2
Fzr1
Ywhah
E2f4
Smc1b
Hdac2
Chek2
Gadd45b
Smc3
Rad21
Cdc23
Cdc7
Wee1
Pkmyt1
Dbf4
E2f1
Tgfb2
Bub3
Orc2
Skp2
Cdkn2c
Ccnd3
Cdk4
Tfdp1
Chek1
Mad1l1
Cdc25a
Bub1b
Bub1
Mcm6
Mad2l1
Mcm3
Cdkn2b
Pcna
Mcm7
Espl1
Orc6
Ccnb2
Cdc25c
Mcm4
Ccna2
Ttk
Mcm2
Cdk1
Plk1
Cdc45
Mcm5
Cdc20
Ccne2
Ccnb1
Ccne1
Orc1
Cdc6
Cdkn1a
Cdkn2a
Akt3
Cd22
Vav3
Nfkbie
Cd72
Cr2
Fcgr2b
Cd79b
Nfat5
Cd19
Pik3ap1
Map2k1
Ppp3ca
Vav2
Jun
Syk
Malt1
Sos2
Ikbkb
Card11
Cd79a
Ptpn6
Ikbkg
Pik3r1
Nfkbia
Blnk
Pik3cd
Rasgrp3
Rac2
Lyn
Gsk3b
Nfatc3
Pik3ca
Sos1
Inpp5d
Bcl10
Akt2
Nfkb1
Nfatc2
Plcg2
Grb2
Dapp1
Rac3
Rela
Kras
Ppp3cb
Chp2
Ppp3r2
Btk
Mapk3
Rac1
Pik3cg
Vav1
Nras
Pik3r2
Pik3r3
Map2k2
Raf1
Cd81
Mapk1
Ppp3cc
Akt1
Nfatc1
Ppp3r1
Chuk
Pik3r5
Ifitm1
Nfkbib
Nfatc4
Fos
Hras
Pik3cb
Cdkn1b
Pold4
Psme2b
Rps27a
Psma8
Gm11808
Uba52
Psme4
Orc4
Psme1
Psmb9
Psmb10
Orc3
Gm21972
Ccna1
Psmb1
Ubc
Pold3
Rb1
Psmb11
Psmd8
Orc5
Psmb8
Rfc1
Rfc2
Gm8394
Gm4950
Ubb
Psme2
Psmd14
Cdk2
Psmd11
Psmf1
Psmd4
Fzr1
Psma7
Psmb2
Psma4
Psma2
Psma5
Psmd5
Pole
Cdt1
Psmd6
Rpa1
Psmc6
Psma1
Psma3
Cdc7
Psmd9
Psme3
Psmd12
Psmd10
Dbf4
Psma6
Psmb7
Psmb4
Gins4
Psmd3
Orc2
Psmc2
Pold2
Psmc1
Psmd7
Psmc4
Psmb5
Gins3
Psmd13
Pola1
Pold1
Psmd2
Psmb6
Psmc5
Pola2
Psmb3
Gins2
Mcm8
Rfc5
Psmc3
Lig1
Rpa2
Fen1
Rfc3
Pole2
Rpa3
Mcm6
Psmd1
Mcm3
Rfc4
Pcna
Mcm7
Orc6
Dna2
Gmnn
Ginsl
Mcm4
Ccna2
Mcm2
Mcm10
Cdc45
Mcm5
Orc1
Cdc6
Cdkn1a
Uvssa
Pold4
Kdm4b
Apbb1
Herc2
Atr
Poli
Hist2h4
Uba7
Rev3l
Rps27a
Rad52
Rad9b
Rnf111
Xrcc4
Histlh4m
Smug1
Xpa
Wrn
Trim25
Gm11808
Uba52
Eya1
Rchy1
Parp1
Sirt6
Nfrkb
Gm28043
Ep300
Mbd4
Hist1h4h
Eya2
Ube2l6
Neil2
Ube2b
Atm
Slx1b
Whsc1
Trp53bp1
Histlh4a
Gm3086
Mnat1
Fan1
Dclre1c
Rmi1
Cul4a
Pnkp
Ino80c
Fancf
Fance
Xpc
Rad51b
Kdm4a
Ino80d
Ino80
Nhej1
Polk
Ercc4
Rad9a
Ube2i
Ercc5
Brca2
Histlh4c
Rev1
Sumo1
Histlh4j
Zbtb32
Rad51d
Histlh4d
Dclre1a
Poll
Actb
Histlh4b
Faap100
Ino80b
Abl1
Ccna1
Yy1
Msh3
Fancc
Ercc2
Mutyh
Usp45
Mpg
Trp53
Ubc
Uimc1
Cul4b
Pold3
Sprtn
Parg
Pias4
Top3a
Actr8
Mapk8
Mapk8
Msh6
Eya3
Usp7
Rhno1
Fam175a
Nthl1
Rfc1
Tceal
Polm
Lig3
Cops2
Brе
Ccnh
Ercc1
Isy1
Cops4
Hist4h4
Actr5
Histlh4f
Spidr
Rfc2
Msh2
Ercc6
Ubb
Mlh1
Xab2
Mcrs1
Cetn2
Mre11a
Polb
Rad50
Xrcc5
Cops7b
Kat5
Gtf2h2
Mdc1
Cops7a
Pms2
Cdk7
Ppp4c
Sumo3
Tfpt
Ddb2
Fancl
Gtf2h3
Cdk2
Zfp830
Neil1
Babam1
Sumo2
Polr2e
Brcc3
Hmgn1
Ppp5c
Histlh4k
Histlh4i
Ufd1l
Rnf168
Cops8
Xrcc1
Nbn
Gtf2h1
Atrip
Fancg
Ercc3
Histlh4n
Chd1l
Rbx1
Polr2d
Polr2b
Apex1
Mus81
Agr
Ube2n
Mad2l2
Rad23b
Ercc8
Rad51c
Gtf2h5
Topbp1
Cops3
Fancm
Rad17
Rbbp8
Hus1
Rad1
Ube2v2
Isg15
Rad18
Polr2i
Polr2k
Gtf2h4
Rif1
Ino80e
Chek2
Rtel1
Ppie
Rpa1
Paxip1
Gps1
Ogg1
Nploc4
Slx4
Polr2j
Cops5
Gm10184
Polr2a
Ddb1
Tdg
Usp10
Cops6
Xrcc6
Rad51ap1
Actl6a
Vcp
Polr2c
H2afx
Polr2h
Usp1
Stral3
Pold2
Blm
Brip1
Polh
Pold1
Dtl
Xrcc2
Chek1
Polr2g
Fancd2
Faap24
Ung
Fanci
Ube2t
Polq
Gen1
Rnf8
Ruvbl1
Palb2
Rfc5
Lig1
Rpa2
Fancb
Fen1
Rfc3
Rpa3
Xrcc3
Rfc4
Pcna
Polr2f
Bard1
Kpna2
Fanca
Dna2
Rmi2
Tipin
Ccna2
Timeless
Exo1
Eme1
Brca1
Rad51
Apitd1
Polr2l
Lig4
Clspn
2810417H13Rik
Usp43
Poln
Rsph10b
Atr
Poli
Rev3l
Top3b
Slx1b
Fan1
Rmi1
Fancf
Polk
Ercc4
Brca2
Rev1
Faap100
Fancc
Wdr48
Telo2
Top3a
Ercc1
Mlh1
Pms2
Fancl
Atrip
Fancg
Gm42641
Mus81
Eme2
Rad51c
Fancm
Rpa1
Slx4
Hes1
Usp1
Stral3
Blm
Brip1
Polh
Fancd2
Faap24
Fanci
Ube2t
Palb2
Rpa2
Fancb
Rpa3
Fanca
Rmi2
Eme1
Brca1
Rad51
Apitd1

Figure S6 (2nd part) (related to Figure 6) Differential expression analyses based on RNA-seq experiments of GC B cells. (**B**) Gene Set Enrichment Analysis (GSEA) heatmap plots for the indicated genesets (see Figure 6B).

A

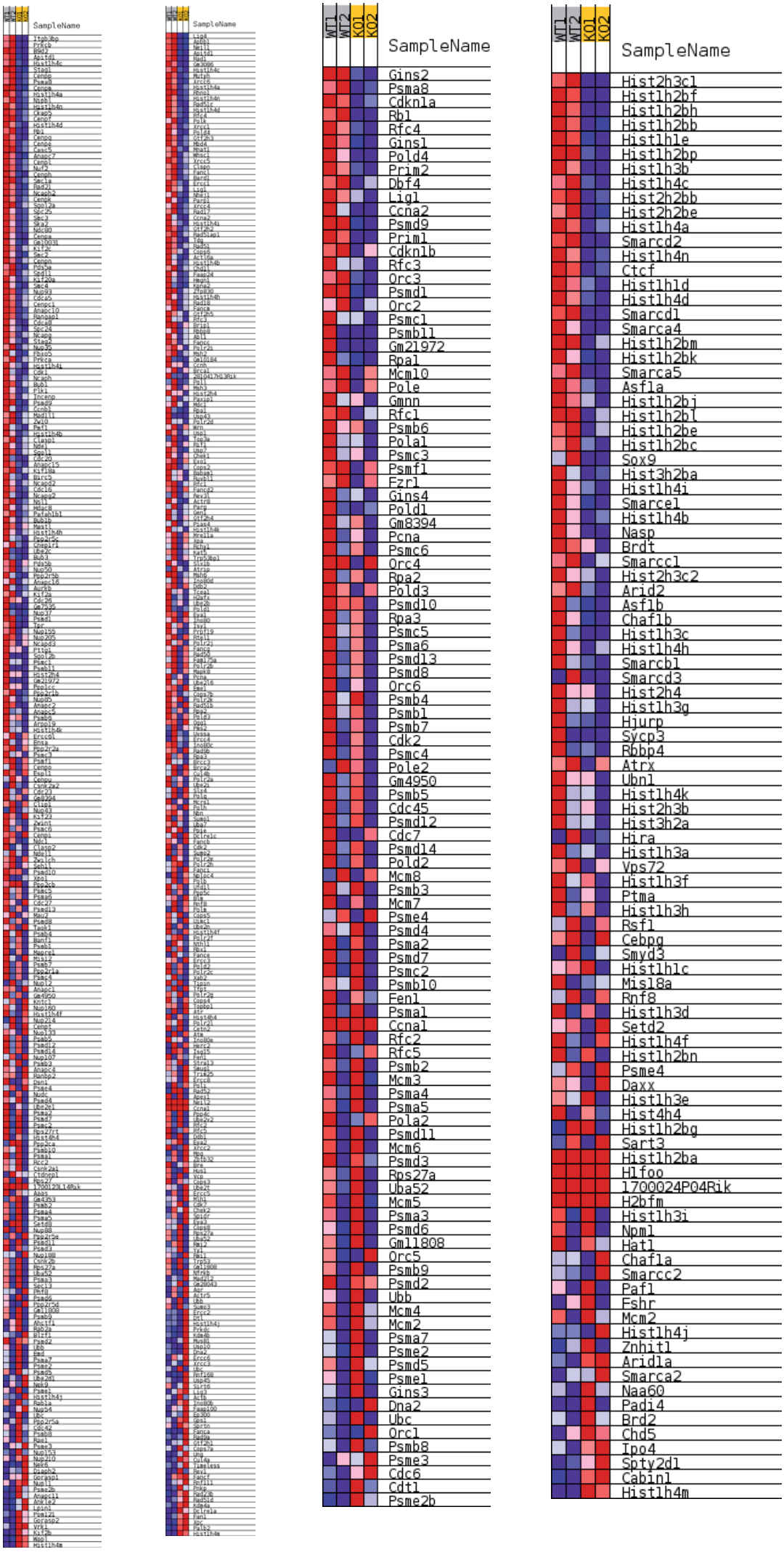
CYCLE M PHASE
DNA REPAIR
DNA REPLICATION
NUCLEOSOME
WT1
WT2
KO1
KO2
SampleName
Gins2
Psma8
Cdknla
Rb1
Rfc4
Ginsl
Pold4
Prim2
Dbf4
Ligl
Ccna2
Psmd9
Priml
Cdknlb
Rfc3
Orc3
Psmd1
Orc2
Psmc1
Psmbll
Gm21972
Rpa1
Mcm10
Pole
Gmnn
Rfcl
Psmb6
Polal
Psmc3
Psmfl
Fzrl
Gins4
Pold1
Gm8394
Pcna
Psmc6
Orc4
Rpa2
Pold3
Psmd10
Rpa3
Psmc5
Psma6
Psmd13
Psmd8
Orc6
Psmb4
Psmbl
Psmb7
Cdk2
Psmc4
Pole2
Gm4950
Psmb5
Cdc45
Psmd12
Cdc7
Psmd14
Pold2
Mcm8
Psmb3
Mcm7
Psme4
Psmd4
Psma2
Psmd7
Psmc2
Psmb10
Fenl
Psmal
Ccnal
Rfc2
Rfc5
Psmb2
Mcm3
Psma4
Psma5
Pola2
Psmdll
Mcm6
Psmd3
Rps27a
Uba52
Mcm5
Psma3
Psmd6
Gmll808
Orc5
Psmb9
Psmd2
Ubb
Mcm4
Mcm2
Psma7
Psme2
Psmd5
Psmel
Gins3
Dna2
Ubc
Orcl
Psmb8
Psme3
Cdc6
Cdtl
Psme2b
Hist2h3cl
Histlh2bf
Histlh2bh
Histlh2bb
Histlhle
Histlh2bp
Histlh3b
Histlh4c
Hist2h2bb
Hist2h2be
Histlh4a
Smarcd2
Histlh4n
Ctcf
Histlhld
Histlh4d
Smarcdl
Smarca4
Histlh2bm
Histlh2bk
Smarca5
Asfla
Histlh2bj
Histlh2bl
Histlh2be
Histlh2bc
Sox9
Hist3h2ba
Histlh4i
Smarcel
Histlh4b
Nasp
Brdt
Smarccl
Hist2h3c2
Arid2
Asflb
Chaflb
Histlh3c
Histlh4h
Smarcbl
Smarcd3
Hist2h4
Histlh3g
Hjurp
Sycp3
Rbbp4
Atrx
Ubnl
Histlh4k
Hist2h3b
Hist3h2a
Hira
Histlh3a
Vps72
Histlh3f
Ptma
Histlh3h
Rsfl
Cebpg
Smyd3
Histlhlc
Misl8a
Rnf8
Histlh3d
Setd2
Histlh4f
Histlh2bn
Psme4
Daxx
Histlh3e
Hist4h4
Histlh2bg
Sart3
Histlh2ba
H1foo
1700024P04Rik
H2bfm
Histlh3i
Npml
Hatl
Chafla
Smarcc2
Pafl
Fshr
Mcm2
Histlh4j
Znhitl
Aridla
Smarca2
Naa60
Padi4
Brd2
Chd5
Ipo4
Spty2dl
Cabinl
Histlh4m

Figure S7 (1st part) (related to Figure 7) Differential expression analyses based on RNA-seq experiments of BM proB cells (**A**) Gene Set Enrichment Analysis (GSEA) heatmap plots for the indicated genesets affecting basic cellular processes (see Figure 7A). (**B**) GSEA heatmap plots for the Ebf1 and Pax5 up- or down-regulated genesets (see Figure 7B,C). (**C**) GSEA analysis and heatmap showing the general downregulation of immunoglobulin genes in *Whsc1*$^{-/-}$ proB cells. (**D**) Sorting strategy and purity of sorted proB cells.

B

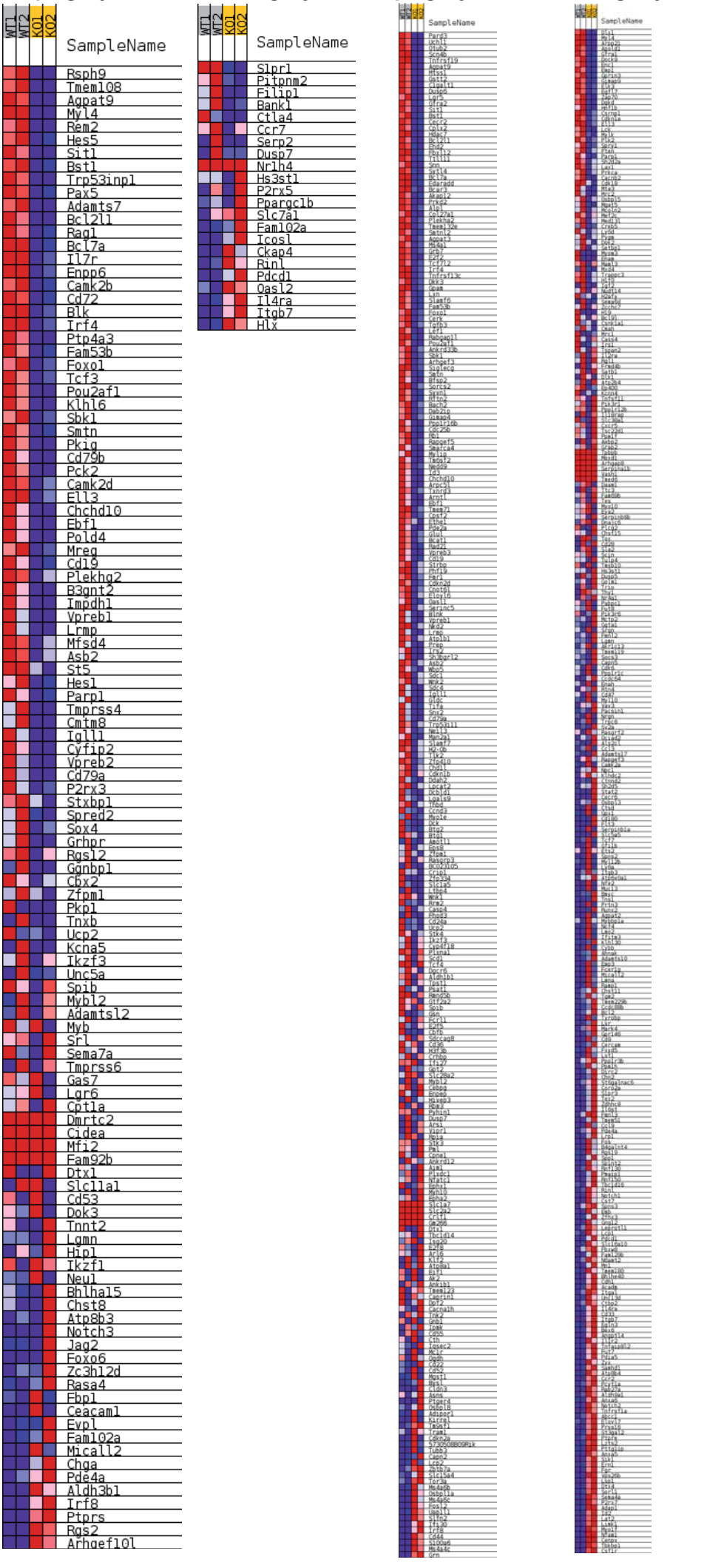

C

GO cc Immunoglobulin Complex

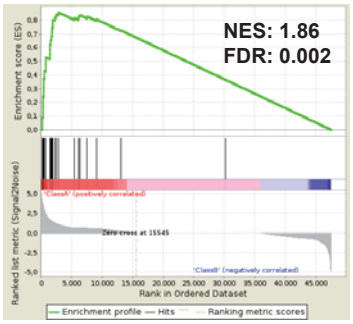

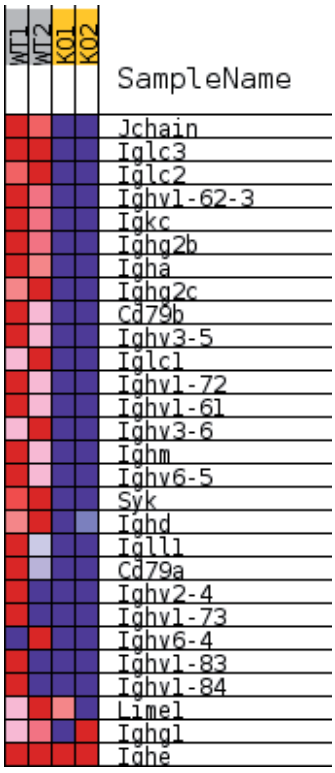

D

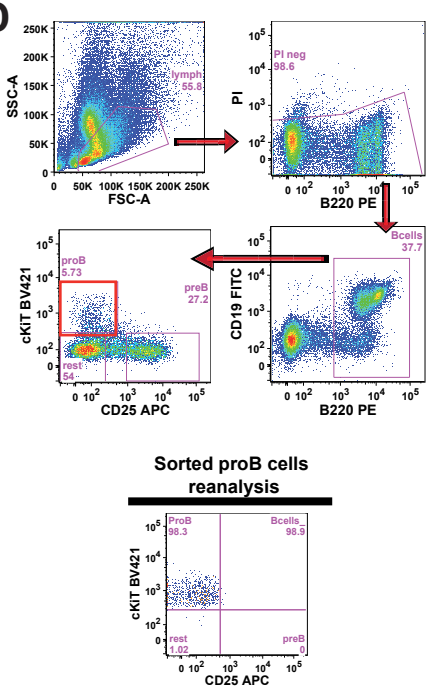

Sorted proB cells reanalysis

Figure S7 (2nd part) (related to Figure 7) Differential expression analyses based on RNA-seq experiments of BM proB cells. (**B**) GSEA heatmap plots for the Ebf1 and Pax5 up- or down-regulated genesets (see Figure 7B,C). (**C**) GSEA analysis and heatmap showing the general downregulation of immunoglobulin genes in *Whsc1*$^{-/-}$ proB cells. (**D**) Sorting strategy and purity of sorted proB cells.

SUPPLEMENTAL EXPERIMENTAL PROCEDURES

Antibodies. The antibodies used in this study were:

	Clone	Fluorochrome	Reference*
Streptavidin		FITC	554060
Anti-BrdU		FITC	347583
CD8a	53-6.7	FITC	Inmunostep-M8AF-05MG
CD4	GK1.5	FITC	553729
CD19	1D3	FITC	553785
CD23	B3B4	FITC	553138
CD44	IM7	FITC	553133
CD71	C2 (=C2F2)	FITC	553266
B220/CD45R	RA3-6B2	FITC	553088
Gr1/Ly6G	RB6-8C5	FITC	553127
IgM	II/41	FITC	553437
IgD	11-26c.2a	FITC	553439
Ly5.1 (CD45.1)	A20	FTIC	553775
Streptavidin		PE	554061
CD3ε	145-2c11	PE	553064
CD4	GK1.5	PE	557308
CD5	53-7,3	PE	552023
CD8a	53-6.7	PE	553033
CD11c	HL3	PE	553802
CD19	1D3	PE	553786
CD21	7G6	PE	552957
CD95/FAS	Jo2	PE	554258
B220/CD45R	RA3-6B2	PE	553090
Gr1/Ly6G	RB6-8C5	PE	553128
Mac1/CD11b	M1/70	PE	553311
Pan-NK cells/CD49b	DX5	PE	553858
TCR-gamma_delta	GL3	PE	553178
Ter119	Ter119	PE	553673
IgM	II/41	PE	eBioscience 12-5790
Anexina V		PE	559763 (kit apoptosis)
Streptavidin		APC	554067
CD8a	53-6.7	APC	553035
CD25	PC61	APC	557192
CD44	IM7	APC	559250
CD117/c-Kit	2B8	APC	553356
B220/CD45R	RA3-6B2	APC	553092
IgD	11-26c	APC	eBioscience 17-5993
IgM	II/41	APC	550676
Mac1/CD11b	M1/70	APC	553312

Ly5.1 (CD45.1)	A20	APC	558701
Ly5.2 (CD45.2)	104	APC	558702
TcrB	H57-597	APC	553174
Streptavidin		PerCP-Cy5.5	551419
B220/CD45R	RA3-6B2	PerCP-Cy5.5	552771
CD25	PC61	PerCP-Cy5.5	551071
CD117/c-Kit	2B8	APCeFluor780	eBioscience 47-1171
Sca1/(Ly-6A/E)	D7	PE-Cy5	eBioscience 15-5981
IL7Rα/CD127	A7R34	PE-Cy7	eBioscience 25-1271
Streptavidin		APC-Cy7	554063
B220/CD45R	RA3-6B2	Pacific Blue	558108
CD4	RM4-5 (L3T4)	Pacific Blue	558107
c-Kit(CD117)	2B8	Violet V-450	560558
c-Kit (CD117)	2B8	Brilliant Violet 421	Biolegend 105827
CD23	B3B4	BIOTIN	553137
CD138/Syndecan	281-2	BIOTIN	553713
Flt3/CD135/Flk2/Ly72	A2F10	Biotin	eBioscience 13-1351
IgA	C10-1	Biotin	556978
IgE	R35-118	Biotin	553419
IgG1	A85-1	Biotin	553441
IgG2a[b]	5.7	Biotin	553504
IgG2b	RMG2b-1	Biotin	Biolegend 406704
IgG3	R40-82	Bitin	553401
IgM	II/41	BIOTIN	553436
Ly5.2 (CD45.2)	104	BIOTIN	553771
Anexina V		BIOTIN	556418 (kit apoptosis)
7-AAD			559763 (Kit apoptosis)
Propidium Iodide, PI			Sigma P4170
CD16/CD32 FcBlock	2.4G2	Purified	553142
PNA (Peanut agglutinin)		FITC	Vector Labs. FL-1071

* BD Biosciences, except otherwise specified

Surface Markers of Hematopoietic Cell types.

Hematopoietic Population	Organ	Markers	Additional information
Hematopoietic Stem/Progenitor Cells (HS/PC)	Bone Marrow	$Lin^{-}Sca1^{hi}c\text{-}Kit^{hi}$	Lineage (Lin) [1]: B220, CD19, CD3ε, CD4, CD8a, DX5,

			Gr1, Mac1, CD11b, and Ter119
Common Lymphoid Progenitors (CLP)	Bone Marrow	Lin^- , $Sca1^{int}$, c-$Kit^{int,}$ $FLT3^+$, $IL7^+$	Lin [1]
Common Myeloid Progenitors (CMP)	Bone Marrow	Lin^- , $Sca1^{neg}$, c-Kit^{hi}	Lin [1]
proB cells	Bone Marrow	$B220^+cKit^+$	
preB cells	Bone Marrow	$B220^+CD25^+IgM^-$	
Immature B cells	Bone Marrow	$B220^{int}IgM^+IgD^-$	
Recirculating B cells	Bone Marrow	$B220^+IgM^{hi}IgD^{low/-}$	
NK cells	Bone Marrow Spleen	$DX5^+$, $TcrB^-$	
Immature B cells	Spleen	$B220^{int}IgM^+IgD^{med}$	
Transitional B cells	Spleen	$B220^+IgM^{hi}IgD^{hi}$	
Mature B cells	Spleen Lymph Nodes	$B220^+IgM^{lo}IgD^{hi}$	
Marginal Zone B cells	Spleen	$B220^+CD21^{hi}CD23^{lo}$	
Follicular B cells	Spleen Lymph Nodes	$B220^+CD21^{int}CD23^{hi}$	
Germinal Center B cells	Spleen Lymph Nodes	$B220^+FAS^{hi}PNA^{hi}$	Additionally if needed, $IgG1^+$ or $IgG3^+$
Double negative thymocytes	Thymus	Lin^-	Lin [2]: CD4, CD8a, Mac1, Gr1, B220, Ter119
Double negative DN1 thymocytes	Thymus	$CD44^+CD25^-$c-Kit^+ Lin^-	Lin [2] Además son $CD3\varepsilon^-$
Double negative DN2 thymocytes	Thymus	$CD44^+CD25^+$c-Kit^+ Lin^-	Lin [2] Además son $CD3\varepsilon^-$
Double negative DN3 thymocytes	Thymus	$CD44^-CD25^-$c-Kit^- Lin^-	Lin [2]
Double negative DN4 thymocytes	Thymus	$CD44^-CD25^-$c-Kit^- Lin^-	Lin [2]
Double positive DP thymocytes	Thymus	$CD4^+$ $CD8^+$	Also $TCR\beta^+$ $CD3\varepsilon^+$ $DX5\alpha^-$
T lymphocytes CD8-SP	Thymus [Médula] Spleen Lymph Nodes Peripheral Blood	$CD4^-$ $CD8^+$	Also $TCR\beta^+$ $CD3\varepsilon^+$ $DX5\alpha^-$

T lymphocytes CD4-SP	Thymus Spleen Lymph Nodes Peripheral Blood	$CD4^+$ $CD8^-$	Also $TCR\beta^+$ $CD3\varepsilon^+$ $DX5\alpha^-$
Granulocytes	Bone Marrow Spleen	$Gr1^{hi}Mac^{hi}$	
Monocytes/ macrophages	Bone Marrow Spleen	$Gr1^{low/int}$ $Mac1^{hi}$	

Sheep Red Blood Cell (SRBC) immunizations. Mice were immunized with 200 µl/mouse of SRBCs (Oxoid SR0051C) resuspended in 1X PBS at a concentration of 10^9 cells/ml, by intraperitoneal injection. SRBCs were washed on 1X PBS at least 3 times before counting them used a handheld automated cell counter, ScepterTM [Millipore®, 40µm tips].

Mouse Embryo Fibroblasts (MEFs) preparation and culture. MEFs were prepared and isolated as previously described (Bermejo-Rodriguez et al., 2006). Each MEF preparation was genotyped by PCR at the moment of obtention (considered passage 1, P1) and the genotype was confirmed at passage 2, when some cells were frozen down. Cells were counted using a handheld automated cell counter, ScepterTM [Millipore®, 60µm tips]. Cell growth curve was measured while keeping the cells at exponential growth and at an under-confluence state. DNA damage response assays were performed by exposing the cells to gamma irradiation at P2 passage.

GC B cells stranded mRNA library preparation and sequencing. MACS-sorted $CD43^-$ splenic B cells were LPS-stimulated for 72h. Cells were not sorted for B cell subpopulations; WT cell samples contained 1.3-fold more follicular B cells than *Whsc1*$^{-/-}$ cells (mean WT FO B cells: 62.07%, SD: 9.61; mean *Whsc1*$^{-/-}$ FO B cells: 46.05%, SD: 9.67; total of n=7 WT vs. n=6 *Whsc1*$^{-/-}$ independent biological replicates were studied). The libraries from the mouse total RNA were prepared using the TruSeq®Stranded mRNA LT Sample Prep Kit (Illumina Inc., Rev.E, October 2013) according to manufacturer's protocol. Briefly, 0.5 µg of total RNA was used for poly-A based mRNA enrichment with oligo-dT magnetic beads. The mRNA was fragmented (resulting RNA fragment size was 80-250nt, with the major peak at 130nt. The second strand cDNA synthesis was performed in the presence of dUTP instead of dTTP, this allowed to achieve the strand specificity. The blunt-ended double stranded cDNA was 3´adenylated and Illumina indexed adapters were ligated. The ligation product was enriched with 15 PCR cycles and the final library was validated on an Agilent 2100 Bioanalyzer with the DNA 7500 assay. The libraries were sequenced on HiSeq2000 (Illumina, Inc) in paired-end mode with a read length of 2x76bp using TruSeq SBS Kit v3-HS. We generated about 50-70 million paired-end reads for each sample in a fraction of a sequencing flowcell lane, following the manufacturer's protocol. Image analysis, base calling and quality scoring of the run were processed using the manufacturer's software Real Time Analysis (RTA 1.13.48) and followed by generation of FASTQ sequence files by CASAVA. Data reported in the manuscript are tabulated in the Supplemental information Tables 1-3 and are available at GEO (GSE84878).

Sorted proB cells mRNA library preparation and sequencing (low input RNA-seq)
RNA sequencing libraries were prepared following the SMARTseq2 protocol (Picelli et al., 2013) with minor modifications. Briefly, RNA was quantified using the Qubit RNA HS Assay Kit (Thermo Fisher Scientific) and 3.2-30.6 ng of RNA was used for cDNA synthesis. Reverse transcription was performed using SuperScrpit II (Invitrogen) in the presence of oligo-$dT_{30}VN$ (1µM; 5′-AAGCAGTGGTATCAACGCAGAGTACT$_{30}$VN-3′), template-switching oligonucleotides (1µM) and betaine (1M). The cDNA was amplified using the KAPA Hifi Hotstart ReadyMix (Kappa Biosystems), 100 nM ISPCR primer (5′-AAGCAGTGGTATCAACGCAGAGT-3′) and 20 cycles of amplification. Following purification with Agencourt Ampure XP beads (1:1 ratio; Beckmann Coulter), product size distribution and quantity were assessed on a Bioanalyzer using a High Sensitvity DNA Kit (Agilent). 200 ng of the amplified cDNA was fragmented for 10 min at 55 ºC using Nextera® XT (Illumina) and amplified for 12 cycles with indexed Nextera® PCR primers. Products were purified twice with Agencourt Ampure XP beads (0.8:1 ratio) and quantified again on a Bioanalyzer using a High Sensitvity DNA Kit. Sequencing of Nextera® libraries was carried out using fraction of a sequencing lane on a HSeq2000 (Illumina inc.) using TruSeq SBS Kit v3-HS, and between 74-80 million paired-end reads

were generated for each sample. The read length was 101bp with TruSeq Dual Index of 8bp+8bp. Images analysis, base calling and quality scoring of the run were processed using the manufacturer's software Real Time Analysis (RTA 1.13.48) and followed by generation of FASTQ sequence files by CASAVA 1.8. are reported in the manuscript are tabulated in the Supplemental information Tables 4-6 and are available at GEO (GSE88970)

Bioinformatic analyses. *Alignment and quantification.* RNA-seq reads were aligned to the mouse reference genome (GRCm38) using STAR (version 2.5.1b)(Dobin et al., 2013) with default ENCODE parameters. For female samples the Y chromosome was removed from the reference before the mapping. Genes were quantified using RSEM (version 1.2.28)(Li and Dewey, 2011) with default parameters. Mouse gene annotation file was downloaded from gencode release vM9 (http://www.gencodegenes.org/). *Differential gene expression.* RSEM gene counts was used as input for the DESeq2 R package (version 1.10.1)(Love et al., 2014) for WT vs KO comparison adding sex as a covariate in the model. DESeq2 was run with default parameters. Genes with FDR<5% were considered significant.
Enrichment Analyses. Gene ontology for biological processes and KEGG pathway enrichment analysis were performed with DAVID db (Huang da et al., 2009). Gene Set Enrichment Analysis was performed with GSEA (Broad Institute) (Subramanian et al., 2005) using the data obtained after normalization and quantification. The use of non-preranked data allows the obtention of heatmaps for the different genesets employed. Preranked analysis was also performed and it corroborated the results obtained (data not shown). For simplicity, only three WT and three *Whsc1*$^{-/-}$ RNA-sequenced samples were used in the GSEA analysis of GC B cells. Normalized Enrichment Scores (NES) and corrected False Discovery Rates (FDR) values are indicated in each plot.

SUPPLEMENTAL REFERENCES

Bermejo-Rodriguez, C., Perez-Caro, M., Perez-Mancera, P.A., Sanchez-Beato, M., Piris, M.A., and Sanchez-Garcia, I. (2006). Mouse cDNA microarray analysis uncovers Slug targets in mouse embryonic fibroblasts. Genomics *87*, 113-118.
Dobin, A., Davis, C.A., Schlesinger, F., Drenkow, J., Zaleski, C., Jha, S., Batut, P., Chaisson, M., and Gingeras, T.R. (2013). STAR: ultrafast universal RNA-seq aligner. Bioinformatics *29*, 15-21.
Huang da, W., Sherman, B.T., and Lempicki, R.A. (2009). Systematic and integrative analysis of large gene lists using DAVID bioinformatics resources. Nat Protoc *4*, 44-57.
Li, B., and Dewey, C.N. (2011). RSEM: accurate transcript quantification from RNA-Seq data with or without a reference genome. BMC Bioinformatics *12*, 323.
Love, M.I., Huber, W., and Anders, S. (2014). Moderated estimation of fold change and dispersion for RNA-seq data with DESeq2. Genome Biol *15*, 550.
Picelli, S., Bjorklund, A.K., Faridani, O.R., Sagasser, S., Winberg, G., and Sandberg, R. (2013). Smart-seq2 for sensitive full-length transcriptome profiling in single cells. Nat Methods *10*, 1096-1098.
Subramanian, A., Tamayo, P., Mootha, V.K., Mukherjee, S., Ebert, B.L., Gillette, M.A., Paulovich, A., Pomeroy, S.L., Golub, T.R., Lander, E.S., *et al.* (2005). Gene set enrichment analysis: a knowledge-based approach for interpreting genome-wide expression profiles. Proc Natl Acad Sci U S A *102*, 15545-15550.